

Prediction of elastic properties of pyrolytic carbon based on orientation angle

Y S Song^{1,2}, L H Qi¹ and Y X Li¹

¹School of Mechatronic Engineering, Northwestern Polytechnical University, Xi'an, China

E-mail: songyongshan@mail.nwpu.edu.cn

Abstract. In the present work, a finite element computation micromechanics model was established to evaluate mechanical properties of pyrolytic carbon (PyC). The proposed computation of PyC considering the texture, i.e. the orientation distribution of the coherent domains, was modeled by a normal distribution that depends on orientation angle (OA). With the proposed model, different textures of PyC, were tested under six different loading modes. The calculated elastic modulus were coincided with the reported experimental results approximately. In particular, the influence of OA of PyC on Young's modulus was investigated. The results show that the Poisson's ratio and Young's module of PyC tend to be isotropic when OA is higher than 110° and the shear modulus becomes isotropic with OA higher than 50°. The results demonstrate that the proposed model would provide a valuable numerical tool to predicate the elastic properties of PyC.

1. Introduction

C/C composites have been widely used for aircraft, aerospace, car and nuclear industry due to their excellent mechanical properties at high temperature [1-2]. Pyrolytic carbon is used as matrix of C/C composites produced by chemical vapor infiltration. In order to predict the mechanical properties of C/C composites, one has to fully investigate the mechanical properties of PyC. Several experimental methods have been used to measure the elastic properties of PyC, such as ultrasonic pulse-echo experiments [3] and sharp indentation tests [4]. But due to the significant anisotropy of PyC, accuracy of the experiment is not satisfied. In order to predict the mechanical properties of PyC, a numerical approach was required.

On the submicron scale, the microstructure of PyC can be described as a set of coherent domains with different orientations. This can be performed by textures, which are classified as: isotropic, low-textured (LT), medium-textured (MT) and high-textured (HT). OA <50°, from 50° to 80°, 80° to 180°, and correspond to HT-, MT- and LT-carbon, respectively[5].

Pyrolytic carbon can be described by a small number of texture components. A texture component is a domain orientation for which the orientation distribution function (ODF) reaches a maximum value. In the neighborhood, the ODF is decreasing in an anisotropic way. A lot of ODF of domains have been reported by different experimental characterization methods [6-8]. However, only Piat [6] utilized the real physical 2D spatial distribution of carbon structural units and established the correlation of ODF and OA.

Micromechanical methods can establish relationship between microstructure and elastic properties and provide all the properties of materials. Micromechanical models for predicting the mechanical properties of pyrolytic carbon have been reported in the literatures [7-9].



It is suggested that the studies for pyrolytic carbon are still insufficient. The investigations of pyrolytic carbon based on orientation angle were rarely studied. The objective of this work is to establish a detailed mechanical model for predicting the elastic properties of pyrolytic carbon with different orientation angles.

The ODF of domains is modeled by a Gauss distribution based on OA. Then, the finite element model is established and the texture is characterized by monte carlo method. In the last part of the paper, the elastic properties with different OA are determined numerically.

2. Model development

The RVE can be regarded as a set of cuboids and shown in Figure 1. Each cuboid represents a coherent domain with same size but different orientations. The unit normal c on each domain can be represented by its endpoint on the sphere around the center O and thus be described by spherical coordinates $\{\sigma, \varphi\}$. The angle φ is distributed in the interval $[0, 2\pi)$ uniformly, and the angle σ corresponds to the Gauss density function [6]:

$$f(\alpha) = (\sigma\sqrt{2\pi})^{-1} \exp(\alpha^2/2\sigma) \quad \sigma \in \left(-\frac{\pi}{2}, \frac{\pi}{2}\right) \quad (1)$$

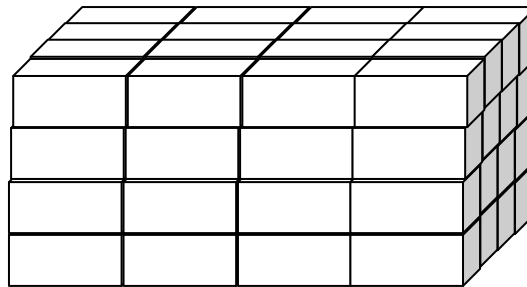


Figure 1. Microstructure of PyC.

The RVE and finite element model is showed in Figure 2 where brick solid element SOLID95 with twenty nodes is used. The finite element approach based on strain energy is finally used to predict effective elastic properties of PyC.

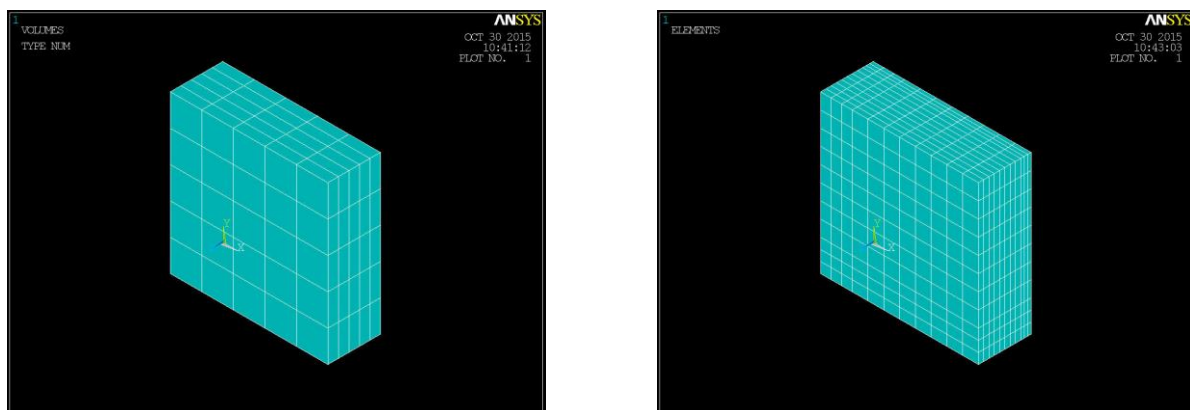


Figure 2. Unit cell and FE mesh.

In this study, special boundary [10-12] conditions are applied on the RVE to evaluate effective elastic properties. The macroscopic behaviors of the RVE can be characterized by the effective stress tensor σ and strain tensor ε in the elastic regime. They are interrelated by the stiffness matrix C^H .

$$\sigma = C^H \varepsilon \quad (2)$$

where $\sigma = \frac{1}{V} \int_{\Omega} \sigma d\Omega$, $\varepsilon = \frac{1}{V} \int_{\Omega} \varepsilon d\Omega$. Consideration the case of 3D orthotropic materials, equation corresponds to

$$\begin{pmatrix} \sigma_x \\ \sigma_y \\ \sigma_z \\ \tau_{yz} \\ \tau_{zx} \\ \tau_{xy} \end{pmatrix} = \begin{pmatrix} C_{11} & C_{12} & C_{13} \\ C_{21} & C_{22} & C_{23} \\ C_{31} & C_{32} & C_{33} \\ & & & C_{44} \\ & & & & C_{55} \\ & & & & & C_{66} \end{pmatrix} \begin{pmatrix} \varepsilon_x \\ \varepsilon_y \\ \varepsilon_z \\ \gamma_{yz} \\ \gamma_{zx} \\ \gamma_{xy} \end{pmatrix} \quad (3)$$

The strain energy of the RVE is equal to:

$$E = \int_{\Omega} \frac{1}{2} (\sigma_{11}\varepsilon_{11} + \sigma_{22}\varepsilon_{22} + \sigma_{33}\varepsilon_{33} + \sigma_{12}\varepsilon_{12} + \sigma_{23}\varepsilon_{23} + \sigma_{31}\varepsilon_{31}) d\Omega - \frac{1}{2} (\overline{\sigma_{11}\varepsilon_{11}} + \overline{\sigma_{22}\varepsilon_{22}} + \overline{\sigma_{33}\varepsilon_{33}} + \overline{\sigma_{12}\varepsilon_{12}} + \overline{\sigma_{13}\varepsilon_{13}} + \overline{\sigma_{31}\varepsilon_{31}}) V \quad (4)$$

Suppose a unit initial strain is imposed in direction 1, i.e. $\varepsilon^{(1)} = (1 \ 0 \ 0 \ 0 \ 0 \ 0)^T$. The corresponding average stress is then obtained by Eq. (4):

$$\overline{\sigma}^{(1)} = (C_{1111}^H \ C_{1122}^H \ C_{1133}^H \ 0 \ 0 \ 0)^T \quad (5)$$

By replacing $\varepsilon^{(1)}$ and $\overline{\sigma}^{(1)}$ in Eq. (5), the strain energy can be obtained as following expression:

$$E^{(1)} = \frac{1}{2} \overline{\sigma}^{(1)} \varepsilon^{(1)} V - \frac{1}{2} C_{1111}^H V \quad (6)$$

The matrix coefficient C_{1111}^H can be derived as:

$$C_{1111}^H = 2E^{(1)} / V \quad (7)$$

3. Results and discussion

The elastic constants $C_{1111} = 40.016$, $C_{3333} = 18.185$, $C_{1122} = 20.021$, $C_{1133} = 12.779$, and $C_{2323} = 1.776$ [GPa] are used for the domains with transversely isotropic material symmetry [4]. In high texture PyC (OA less than 50°), Taylor et al.[13] performed nanoindentation tests (Berkovich indenter) perpendicular to deposition direction and the measured values of Young's modulus were between 16.1 and 26.2 GPa. These values were in good agreement to the calculated elastic modulus (between 18.4 and 26.5 GPa).

The predicted extensional (EX and EZ) modulus of the pyrolytic carbon with various values of OA are presented in Figure 3. It is observed that with the increase of OA, EX is decreased while EZ is slight decreased firstly, and then increases. However, when $OA > 110^\circ$ the influence of OA on EX and EZ seems negligible. It can be found that When $OA > 110^\circ$, PyC tends to be an isotropic material. The effect of the OA of PyC on its microstructure is quite significantly.

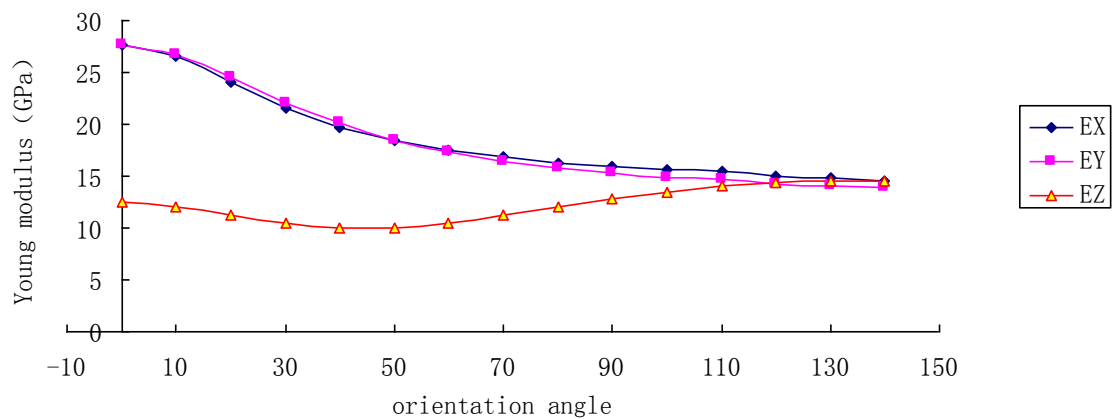


Figure 3. Young's moduli with different orientation angles.

The predicted shear (GXY and GYZ) moduli of the PyCs are presented in Figure 4. It is observed that when $OA > 50^\circ$, PyC tends to an isotropic material. With the increase of OA, GXY is decreased from 10 to 4.5 Gpa while GYZ is increased from 2 to 4 Gpa.

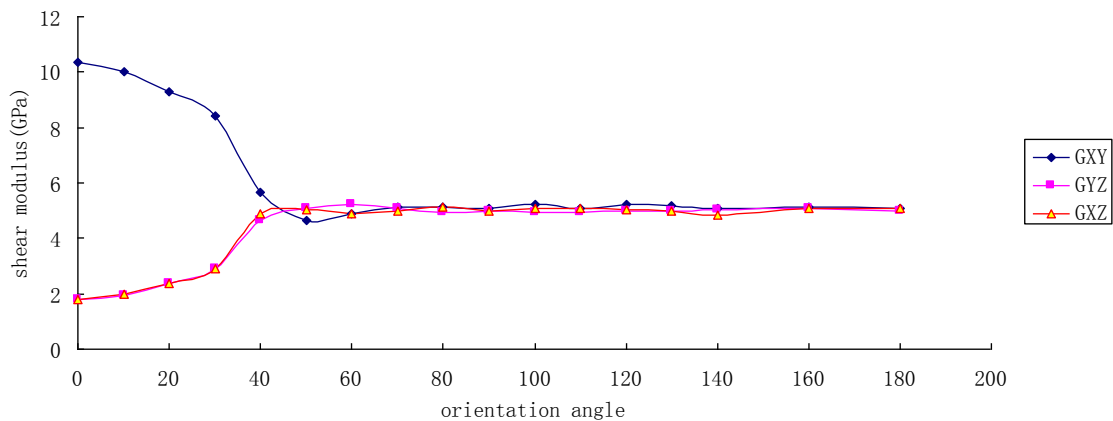


Figure 4. Shear moduli with different orientation angles.

Values of the Poisson's ratio with different OA are presented in Figure 5. When $OA < 50^\circ$, V_{xy} decreases firstly, and then increase with the increase of OA, V_{xz} and V_{yz} have an opposite tendency. PyC tends to be isotropic in poisson ratio with $OA > 110^\circ$.

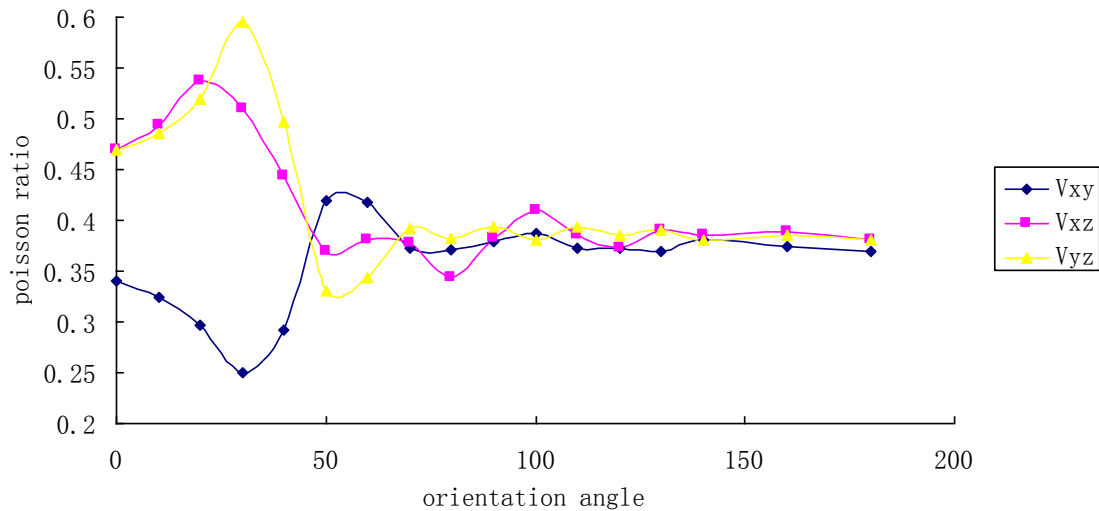


Figure 5. Poisson ratio with different orientation angles.

4. Conclusions

The elastic properties of PyC on the micrometer scale have been determined based on the elastic properties of the domains and the orientation distribution of the domains. A Gauss distribution function based on OA has been used as a texture component model.

A numerical study of PyC using ANSYS was performed. The numerical results indicate that the strong elastic anisotropy of PyC induces a large gap, and it is found that the HT pyrolytic carbon films and measured values of Young's modulus between 16.1 and 26.2 GPa. These values are in good agreement to the calculated elastic moduli (between 18.4 and 26.5 GPa). The bounds and the approximations of the effective elastic properties depend only on one concentration parameter which completely specifies OA.

There are significant gradients in the elastic properties of the material throughout the whole domain of the values for OA and thus throughout the different texture degrees of HT, MT and LT. PyC tends to be the Poisson ratio and Young's modulus of an isotropic material with $OA > 110^\circ$, shear moduli of which with $OA > 50^\circ$.

Acknowledgements

This work has been supported by the National Natural Science Foundation of China under Grant No.50472203 and the Doctorate Foundation of Northwestern Polytechnical University.

References

- [1] Reznik B and Huttinger K J 2002 On the terminology for pyrolytic carbon *Carbon* **40**(4) 621-4
- [2] Reznik B, Gerthsen D and Huttinger K J 2001 Micro- and nanostructure of the carbon matrix of infiltrated carbon fiber felts *Carbon* **39**(2) 215-9
- [3] Gebert J M *et al* 2010 Elastic constants of high-texture pyrolytic carbon measured by ultrasound phase spectroscopy *Carbon* **48**(12) 3647-50
- [4] Diss P, Lamon J, Carpentier L, Loubet J and Kapsa P 2002 Sharp indentation behavior of carbon/carbon composites and varieties of carbon *Carbon* **40**(14) 2567-79
- [5] Papadakis E P and Bernstein H 1963 Elastic moduli of pyrolytic graphite *J. Acoustical Sci. America* **35**(4) 521-4
- [6] Piat R, Reznik B, Schnack E and Gerthsen D 2004 Modeling of effective material properties of pyrolytic carbon with different texture degrees by homogenization method *Compos. Sci. Technol.* **64** 2015-20

- [7] Sauder C and Lamon J 2005 Prediction of elastic properties of carbon fibers and CVI matrices *Carbon* **43**(10) 2044-53
- [8] Sauder C, Lamon J and Pailler R 2005 The tensile properties of carbon matrices at temperatures up to 2200° *Carbon* **43**(10) 2054-65
- [9] Böhlke T, Jöchen K, Piat R, Langhoff T A, Tsukrov I and Reznik B 2010 Elastic properties of pyrolytic carbon with axisymmetric textures *Tech. Mech.* **30**(4) 343-53
- [10] Rao M V, Mahajan P and Mittal R K 2008 Effect of architecture on mechanical properties of carbon/carbon composites *Compos. Struct.* **83** 131-42
- [11] Swain M V and Field J S 1996 Investigation of the mechanical properties of two glassy carbon materials using pointed indenters *Philos. Mag. A.* **74** 1085-96
- [12] Richter A, Ries R, Smith R, Henkel M and Wolf B 2000 Nanoindentation of diamond, graphite and fullerene films *Diamond Relat. Mater.* **9** 170-84
- [13] Taylor C, Wayne W and Chiu W 2003 Residual stress measurement in thin carbon films by raman spectroscopy and nanoindentation *Thin Solid Films* **429**(1-2) 190-200